Journal of Ovarian Research

RESEARCH

Open Access

MSCs–derived EVs protect against chemotherapy-induced ovarian toxicity: role of PI3K/AKT/mTOR axis

Nehal M. Elsherbiny[1*], Mohamed S. Abdel-Maksoud[2], Kousalya Prabahar[3], Zuhair M. Mohammedsaleh[4], Omnia A. M. Badr[5], Arigue A. Dessouky[6], Hoda A. Salem[3], Omnia A. Refadah[7], Ayman Samir Farid[8], Ashraf A. Shamaa[9] and Nesrine Ebrahim[10,11,12,13*]

Abstract

Chemotherapy detrimentally impacts fertility via depletion of follicular reserves in the ovaries leading to ovarian failure (OF) and development of estrogen deficiency-related complications. The currently proposed options to preserve fertility such as Oocyte or ovarian cortex cryopreservation are faced with many technical obstacles that limit their effective implementation. Therefore, developing new modalities to protect ovarian function remains a pending target. Exosomes are nano-sized cell-derived extracellular vesicles (EVs) with documented efficacy in the field of regenerative medicine. The current study sought to determine the potential beneficial effects of mesenchymal stem cells (MSCs)-derived EVs in experimentally induced OF. Female albino rats were randomly allocated to four groups: control, OF group, OF + MSCs-EVs group, OF + Rapamycin (mTOR inhibitor) group, and OF + Quercetin (PI3K/AKT inhibitor) group. Follicular development was assessed via histopathological and immunohistochemical examination, and ovarian function was evaluated by hormonal assay. PI3K/Akt/mTOR signaling pathway as a key modulator of ovarian follicular activation was also assessed. MSCs-EVs administration to OF rats resulted in restored serum hormonal levels, preserved primordial follicles and oocytes, suppressed ovarian PI3K/AKT axis and downstream effectors (mTOR and FOXO3), modulated miRNA that target this axis, decreased expression of ovarian apoptotic markers (BAX, BCl2) and increased expression of proliferation marker Ki67. The present study validated the effectiveness of MSCs-EVs therapy in preventing ovarian insufficiency induced by chemotherapy. Concomitant MSCs-EVs treatment during chemotherapy could significantly preserve ovarian function and fertility by suppressing the PI3K/Akt axis, preventing follicular overactivation, maintaining normal ovarian cellular proliferation, and inhibiting granulosa cell apoptosis.

Keywords Fertility preservation, Chemotherapy, Ovaries, MSCs-derived exosomes, PI3K/Akt/ mTOR

*Correspondence:
Nehal M. Elsherbiny
nelsherbiny@ut.edu.sa
Nesrine Ebrahim
Nesrien.salem@fmed.bu.edu.eg

Full list of author information is available at the end of the article

MSCs–derived EVs protect against chemotherapy-induced ovarian toxicity: role of PI3K/AKT/mTOR axis.

Introduction

Annually, cancer affects more than 6.6 million women worldwide, with 10% of those affected being under 40 [1]. The significant advancements in cancer diagnosis and treatment result in increased survival rates of cancer patients. Unfortunately, these remarkable results achieved through treatments are accompanied by deleterious impacts on reproductive function. In this context, women's chances of getting pregnant drop by approximately 38% following a cancer diagnosis and course of treatment [2]. Chemotherapy induces direct toxicity to ovaries. Indeed, chemotherapy triggers apoptosis of growing follicles and depletion of the primordial follicular reserve. Also, it can cause damage to the ovarian vasculature, inflammation, direct loss, or accelerated activation of primordial follicles. All these events lead to primary ovarian insufficiency (POI), an established long-term side effect in female cancer survivors in which both endocrine and reproductive ovarian function are disrupted [3]. The primary factors that determine the extent of ovarian damage are the class of chemotherapeutic agent, its dosage, and the course of treatment [4]. In addition to infertility, estrogen deficiency associated with ovarian dysfunction leads to compromised quality of life, deteriorated bone function, neurological and cardiovascular diseases [5].

Several fertility preservation (FP) techniques, including cryopreservation of the ovarian cortex or cryopreservation of oocyte or embryo with or without stimulation of the ovary, are proposed to protect the gametes from the toxic consequences of chemotherapy. Nonetheless, age and health conditions may limit the use of these methods. Furthermore, these procedures are technically challenged, invasive, expensive, and unaffordable for many patients [6]. Moreover, the concept of FP is limited by ethical, and/or religious concerns in many countries [7]. Thus, preventing chemotherapy-induced POI may be a worthwhile option for young cancer survivors to maintain their best chances of conceiving naturally or with medical assistance [8].

The mammalian follicular reserve in the ovary is composed of primordial follicles. This reserve develops early in life and gradually diminishes over the course of the reproductive period [9]. Predominantly quiescent primordial follicles must be preserved, and their activation into early-growing follicles must be consistently suppressed to preserve female reproductive function. Primordial follicles' activation begins during fetal life and is meticulously regulated by balancing stimulatory and inhibitory factors. These factors are released by oocytes and/or granulosa cells and include cytokines, growth hormones, and transcription factors which work in an endocrine, auto-, or paracrine manner to modulate follicular activation [10]. When the primordial follicle pool is depleted, ovarian senescence or menopause occurs, which in turn results in infertility [11].

Numerous studies have emphasized the essential role of the phosphatidyl-inositol-3-kinase (PI3K)–Akt–mammalian target of rapamycin (mTOR) signaling pathway in regulating primordial follicles activation, survival, atresia, and loss in oocytes [12, 13]. The activity of mTOR is increased in oocytes, underscoring the pivotal role of this protein in the activation of primordial follicles. However, accelerated mTOR activity by deletion of its negative regulators PTEN or TSC1 in mice resulted in the activation of primordial follicles entire pool with subsequent POI [14]. Additionally, inhibition of PI3K/Akt/mTOR signaling preserved the follicle pool and prevented chemotherapy-induced ovarian insufficiency [15]. These studies highlight the importance of maintaining balanced PI3K/Akt/mTOR signaling for normal ovarian functioning. The PI3K/Akt/mTOR pathway is implied to be a critical regulator of typical follicular activation. However, under pathological conditions, this axis is dysregulated leading to exacerbation of follicular activation, and exhaustion of the entire follicle pool, leading to premature ovarian failure (POF) phenotype.

Exosomes are lipid membrane-surrounded nanoparticles that have a diameter of less than one micrometer and carry the cytoplasmic components of the cells producing them. Through surface-expressed ligands and receptors, exosomes can deliver their cargo which includes nucleic acids, proteins, and bioactive lipids to target cells, changing their function and phenotype [16, 17]. In vitro and in vivo studies have shown the reparative and protective effects of mesenchymal stem cells (MSCs)-derived exosomes on various tissues. Transplanting exosomes is thought to be a novel cell-free therapeutic approach for treating a variety of degenerative disorders [18]. Interestingly, MSCs-EVs have demonstrated considerable potential for regulating diverse cellular pathways, including the PI3K/mTOR/AKT pathway. This inhibition may offer therapeutic benefits, especially in disorders where the mTOR/AKT pathway is frequently dysregulated such as ulcer colitis [19], sepsis [20], keloids [21], and Alzheimer's disease [22]. Consequently, the goal of this study is to determine how beneficial bone marrow MSCs-EVs are for protecting rats' ovaries against dysfunction caused by chemotherapy and to unravel the impact of MSCs-EVs on PI3K/AKT/mTOR axis signaling, a key pathway in modulating ovarian follicular survival and activation. The effect of MSCs-EVs was tested in comparison to rapamycin as mTOR inhibitor [15], and quercetin as PI3K/AKT inhibitor [23] on OF induced experimentally using Busulfan and cyclophosphamide chemotherapy.

Materials and methods

Experimental animals

Six-week-old, sexually mature female albino rats weighing 180–200 g and in the diestrus (DE) phase were obtained from the Experimental Animal Unit of the Faculty of Veterinary Medicine, Benha University, Egypt, and were acclimatized for 2 weeks under standard laboratory conditions. Every day, vaginal smears were used to examine the various stages of the estrus cycle. Sterile cotton swabs dipped in phosphate buffer saline (PBS) were used to prepare the vaginal swabs, which were subsequently fixed in absolute methanol. Following fixation, the smears of swabs were stained with Giemsa, and assessed under a microscope (Nikon, Japan). Animals were bred and raised in pathogen-free cages and were exposed to room temperature (23±3 °C) and a standard 12-hour light/dark cycle beginning at 8:00 AM. They were also allowed unrestricted access to clean water and food.

Source and localization of lyophilized MSCs-derived extracellular vesicles (MSCs-EVs)

Lyophilized MSCs-EVs powder (Bioluga ® Canada) was reconstituted in distilled water, and each 1 ml of the MSCs-EVs was derived from 0.5×10^6 MSCs. Immunohistochemistry staining for CD105 was performed to localize administrated MSCs-EVs in ovarian tissues.

Ovarian failure (OF) induction

Busulfan (Sigma-Aldrich, Missouri, B2635, 10 mg/kg) was administrated to rats every day for 4 days, and for the first 2 days, they were given daily 100 mg/kg cyclophosphamide (Baxter, India) [24]. Histological and hormonal assessments were used to confirm OF after 4 weeks of induction. Dimethyl sulfoxide (DMSO, Sigma-Aldrich) was diluted (1:1) with sterile water and used to dissolve busulfan to be administered intraperitoneally (i.p.). One to two hours after the busulfan injection, cyclophosphamide dissolved in sterile injection-grade water was i.p. administered.

Experimental design

The timeline of treatments is indicated in Fig. 1. Fifty animals were randomly grouped into five groups as follows ($n=10$):

Control group

Animals received sterile injection grade water i.p. and DMSO diluted with water (1:1) for the first 2 days. Then, the diluted DMSO was continued for a further 2 days. Animals were left untreated for 4 weeks. After that, PBS was i.p. administrated for 6 weeks.

OF group

After 4 weeks of OF induction, rats were intraperitoneally injected with PBS for 6 weeks.

OF + MSCs-EVs group

MSCs-EVs were intraperitoneally injected (as a single dose) 1 week before induction of OF and then after 4 weeks of induction; 2 doses of MSCs-EVs, were intraperitoneally injected 2 weeks apart, then the experiment was ended 4 weeks after the second MSCs-EVs injection. For every animal, 0.5 ml of MSCs-EVs at a concentration of

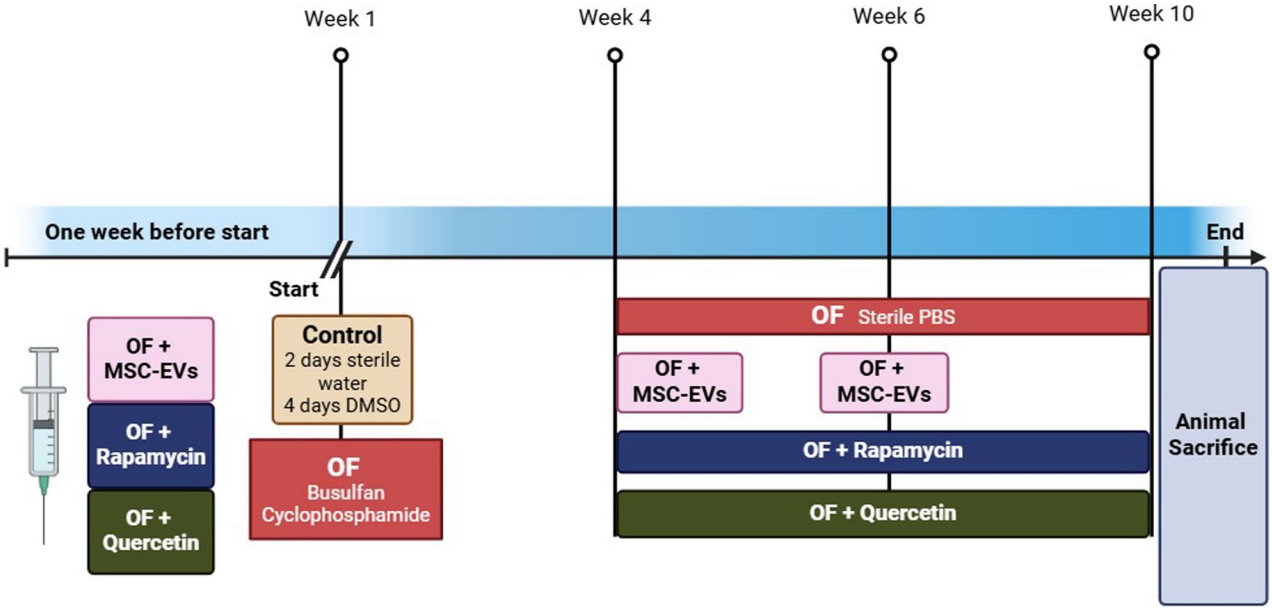

Fig. 1 Schematic presentation of the timeline of treatments

100 µg protein/ml was administered [24]. The number and times of injections were selected based on previous studies [25] and preliminary experiments.

OF + rapamycin group

Rapamycin (8 mg/kg) was administrated daily 1 week before OF induction. Then, 4 weeks after OF induction, rats were intraperitoneally injected daily for 6 weeks with rapamycin [15].

OF + quercetin group

Rats were injected with daily Quercetin (40 mg/kg) 1 week before OF induction. Then, 4 weeks after OF induction, rats were intraperitoneally injected daily for 6 weeks with Quercetin [26].

It should be noted that the current study is limited by the lack of an MSCs-EVs-only treatment group to test the safety of MSCs-EVs and rule out any tumorigenic effects.

Sample collection

Rats were fasted for 12 h at the end of the experimental period before receiving 10 mg/kg xylazine and 100 mg/kg ketamine by intramuscular injection to induce anesthesia. The blood was then withdrawn from the retro-orbital sinus using a capillary tube. Blood samples were used to prepare serum which was further used to assess gonadal hormones. Ovarian tissue samples were dissected and divided into three parts. The first part was fixed in formaldehyde 10% to be processed as paraffin blocks for histopathological and immunohistochemical studies. The second and third parts were processed to be used for biochemical and molecular analyses.

Table 1 Sequences of primers for target genes and miRNA used

Gene/miRNA	Sequence		Accession number
PTEN	Forward	AGACCATAACCCAC CACAGC	NM_031606.2
	Reverse	TCACCTTTAGCTGG CAGACC	
FOXO3	Forward	GCCTCATCTCAAAG CTGGGT	NM_001106395.1
	Reverse	AGTTCTGCTCCACG GGAAAG	
GAPDH	Forward	TGCTGGTGCTGAGT ATGTCG	NM_017008.4
	Reverse	TTGAGAGCAATGC CAGCC	
miR-200c	Forward	GTTTG CGTCTTACC CAGCA	MIMAT0017150
	Reverse	GTGCAGGGTCCG AGGT	
miR-122	Forward	GTGTGGAGTGTGAC AATGG	MIMAT0000827
	Reverse	GTGCAGGGTCCG AGGT	
miR-99	Forward	GTGAACCCGTAGAT CCGAT	MIMAT0000820
	Reverse	GTGCAGGGTCCG AGGT	
U6	Forward	CTCGCTTCGGCAG CACA	XR_004936894
	Reverse	AACGCTTCACGAAT TTGCGT	

Gene expression profile

To extract total RNA from ovarian tissues, TRIzol (Invitrogen) was used according to the manufacturer's instructions. For extraction and purification of miRNA, mirPremier microRNA isolation Kit (Sigma Aldrich, USA) was used. Using a Nano-Drop 2000 C spectrophotometer (Thermo Scientific, USA), the extracted RNA was tested for concentration and purity. A high level of RNA purity was considered at an A260/A280 absorbance ratio exceeding 1.9. The SensiFast cDNA synthesis kits (Sigma Bioline, UK) for RNA and the NCode VILO miRNA cDNA Synthesis Kit (Invitrogen, USA) for miRNA were used to synthesize complementary DNA (cDNA), following the manufacturer's protocol. Next, quantitative PCR (qPCR) was performed using Maxima SYBR Green/ROX qPCR master mix (2x) (Thermo Scientific, USA). Table 1 indicates the sequence of primers used in this study. GAPDH and U6 were used for normalization. For the calculation of the relative gene expression ratios, the formula: $RQ = 2^{-\Delta\Delta Ct}$ was used [27].

Western blot

Ovarian tissue protein was extracted from different experimental groups. Laemmli buffer was added to protein samples followed by heating for 5 min at 95 °C. Then, 50 mg of protein samples were loaded onto sodium dodecyl sulfate (SDS, 10%) polyacrylamide gels followed by electrophoretic resolution. For blotting, the protein was then transferred to a polyvinylidene difluoride (PVDF) membrane (Millipore, Merk, Germany). The blots were blocked by 1-hour incubation in 5% nonfat dry milk in 0.1% TBS/Tween 20. Next, the blots were incubated with the appropriate primary antibodies for an entire night at 4 °C, PTEN (E-AB-63495, Elabscience, USA), FOXO3 (NBP2-16521, Novus Biologicals USA), mTOR (sc-517464, Santa Cruz Biotechnology, USA), Phospho-mTOR (sc-293133, Santa Cruz Biotechnology, USA), PI3K (E-AB-64202, Elabscience, USA), Phospho-PI3K (E-AB-20966, Elabscience, USA), AKT (E-AB-15441, Elabscience, USA), Phospho-AKT (E-AB-20804, Elabscience, USA), β-actin (E-AB-20031, Elabscience, USA). The blots were then washed before incubation with appropriate alkaline phosphatase (ALP) conjugated secondary antibody at room temperature for 1 h. For visualization of the protein bands, a BCIP/NPT detection kit (BWR1067, Biospes, China) was used, and for

densitometric analysis, ImageJ® software was applied. To ensure normality, β-actin was employed as a housekeeping protein.

Enzyme-linked immunosorbent assay (ELISA) for AMH, FSH, LH, and E2

Estradiol (E2, CSB-E05110r, Cusabio Biotech, USA), Follicle-Stimulating Hormone (FSH, CSB-E06869r, Cusabio Biotech, USA), Luteinizing Hormone (LH, CSB-E12654r, Cusabio Biotech, USA), and anti-Müllerian hormone (AMH, CSB-E11162r, Cusabio Biotech, USA) were measured in serum using commercially available ELISA kits in line with the guidelines provided by the manufacturer.

Analysis of molecular interaction network and targeted pathways

The analysis of the PTEN and FOXO3 genes was conducted through integrated transformation and correlation assessments using FunRich software (version 3.3; http://www.funrich.org/). This analysis aimed to elucidate molecular interaction networks and biological pathways, applying a statistical significance threshold of $P<0.05$. Additionally, to evaluate the implication of specific exosomal miRNAs, including miR-200c, miR-122, and miR-99, FunRich was employed for molecular pathway enrichment analysis, again using the same $P<0.05$ threshold. This comprehensive approach allowed for a detailed exploration of the functional roles of the studied genes and miRNAs in the context of ovarian toxicity and their potential therapeutic implications.

Histopathological analysis

Haematoxylin and eosin (H&E) staining

Ovarian sections of 4-6-µm-thickness were prepared from fixed ovarian tissue specimens. For the dehydration of fixed sections, ascending concentrations of ethanol were used. After two rounds of distilled water washing, the dehydrated sections were stained with H&E. Using a light microscope (Leica DMR 3000; Leica Microsystem), Ovarian tissue sections were inspected and analyzed, and images were captured by two experienced investigators who were blinded to the process [28].

Immunohistochemistry analysis

Deparaffinized sections were hydrated, and then H_2O_2 (10%) was used to block endogenous peroxidase activity. The sections were then incubated with primary antibodies after being blocked for nonspecific reactions. The primary antibodies used were Anti-Ki67 antibody [SP6], (ab16667), Rabbit monoclonal [SP6] to Ki67, 1/200, Abcam), Anti-Bax antibody [E63] (ab32503), Rabbit monoclonal [E63] to Bax, 1/250, abcam, Anti-Bcl2-L-13 antibody [EP10625] (ab203516), Rabbit monoclonal [EP10625] to Bcl2-L-13, 1/500, Anti-CD105 antibody (Anti-CD105 antibody [8A1], ab230925) to CD105. Before incubating with the biotinylated secondary antibody, the slides were washed with PBS. After that, the slides were incubated with labeled avidin-biotin peroxidase, employing diaminobenzidine as a chromogen to visualize the antigen-antibody reaction.

Morphometric study

Scoring of immunoreactivity was performed with the Allred score, which provides a 0–8 scale representing Allred index (0–1 = negative, 2–3 = mild, 4–6 = moderate, and 7–8 = strongly positive) [29]. Using the QuPath program (0.1.2), the percentage of positive cells and staining intensity grades (0–3) are added to determine the score [30]. Also, the number of primordial follicles (healthy and atretic) was assessed.

Statistical analysis

GraphPad Prism, version 8 (GraphPad Software) was used for data analyses and presentation. Results were presented as mean ± standard error of mean (SEM). Statistical analysis was performed by applying one-way ANOVA test. Post-hoc analysis was then performed using Tukey's test. The significance was considered at a P value less than 0.05.

Results

CD105 immunostaining

CD105 is a marker of MSCs. MSCs-EVs express specific surface markers of MSCs on their surface [31]. The positive immunoexpression for CD105 in the MSCs-EVs treated group indicated that the MSCs-derived EVs were

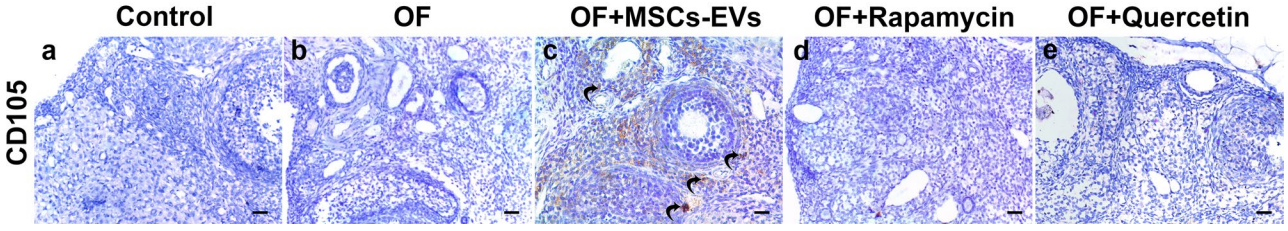

Fig. 2 Representative photomicrographs of CD105 (MSCs marker) immuno-stained sections. The positive immunoexpression for CD105 was observed in MSCs-EVs treated group

localized in the ovarian tissues, Fig. 2. The use of CD105 as sole marker for localization is one of the study's limitations. While CD105 is a widely accepted marker for MSCs, it may not fully capture the complexity of exosome localization within tissues. Studying additional markers or applying advanced imaging techniques could provide a more comprehensive assessment.

Preservation of ovarian structure and hormonal balance by MSCs-derived EVs

Histopathological examination revealed the impact of chemotherapy on follicular development and ovarian structure and how MSCs-EVs reverse this effect. The examination of H&E-stained sections of the control group revealed normal ovarian histoarchitecture. Ovarian follicles in various stages of development, in addition to corpus luteum and blood vessels were seen Fig. 3a &b. While, following the chemotherapeutic treatment in the OF group, marked alterations, most notably extensive atresia of the follicles and degenerated follicles were observed. Furthermore, numerous areas of hemorrhage were found throughout the ovarian tissue, Fig. 3c&d. In the OF+MSCs-EVs group, the administration of EVs led to a marked improvement in ovarian alterations. The ovarian follicles and the overall histoarchitecture neared that of the control group, Fig. 3e &f. Concerning OF+rapamycin and OF+quercetin groups, fewer atretic follicles were observed in both groups, however, developing follicles were more numerous in group IV, Fig. 3g& h. Dilated congested blood vessels and persisted in both groups, Fig. 3g&h and i&j. So, the OF group exhibited a significant decrease in the number of primordial follicles and oocytes, indicating chemotherapy-induced damage to the ovarian reserve. In contrast, the MSCs-EVs treated group showed preservation of primordial follicles and oocytes, suggesting a protective effect of MSCs-EVs on follicular reserve and development.

Simultaneously, a hormonal assay was conducted to assess the effect of MSCs-derived EVs on ovarian function. As shown in Fig. 4, the OF group demonstrated a significant decrease in E2, and AMH ($P<0.0001$) but a marked increase in FSH ($P<0.001$) and LH ($P<0.0001$) compared to the control group, indicating ovarian dysfunction. Conversely, MSCs-EVs administration markedly restored serum E2, AMH ($P<0.0001$) and decreased serum FSH ($P<0.001$) and LH ($P<0.0001$) compared to the OF group. The effect of MSCs-EVs was more favorable when compared to either rapamycin or quercetin treatment. These results suggest a protective effect of MSCs-derived EVs on hormone production and ovarian function.

Effect of MSCs-EVs on modulation of PI3K/AKT/mTOR axis

As shown in Fig. 5A, ovarian gene expression of PTEN, an inhibitor of PI3K/AKT, in the OF group is significantly decreased ($P<0.01$) compared to the control group. In contrast, MSCs-EVs treatment markedly restored gene expression of PTEN level in ovarian tissue ($P<0.001$) compared to the OF group. Meanwhile, rapamycin treatment significantly increased ovarian PTEN expression ($P<0.01$), however, the quercetin-treated group demonstrated a non-significant increase in ovarian PTEN expression compared to the OF group. Similarly, western blot analyses demonstrated a marked decrease in the ovarian PTEN in the OF group ($P<0.0001$) compared to the normal control group. Treatment with MSCs-EVs and rapamycin markedly restored PTEN levels compared to the OF group ($P<0.0001$, $P<0.001$), Fig. 5C, D, respectively. Moreover, gene expression of FOXO3, a downstream effector of PI3K/AKT pathway was markedly increased in the OF group compared to the normal control group ($P<0.001$). MSCs-EVs and rapamycin treatment markedly reduced the gene expression of FOXO3 in ovarian tissue compared to the OF group

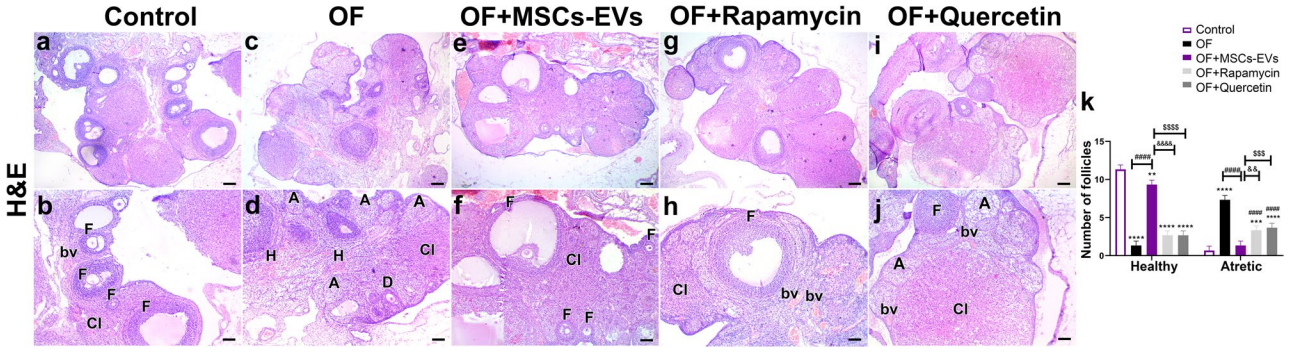

Fig. 3 Representative photomicrographs of H&E-stained sections: **a, b)** Group I: Ovarian follicles (F) in various stages of development, and blood vessels (bv). **c, d)** Group II: extensive atresia of the follicles, with shrunken darkly stained nuclei (A), dilated congested blood vessels (bv), areas of hemorrhage (H), and degenerated follicles (D). **e, f)** Group III: Normal ovarian architecture, with developing follicles (F), blood vessels (bv), and corpus luteum (CL), **g, h** and **i, j)** Group IV and V: Fewer atretic follicles (A) in both groups with more numerous developing follicles (F) in Group IV. Persistent dilated congested blood vessels (bv) are noticed in both groups. **k)** Histogram demonstrating ovarian follicle count

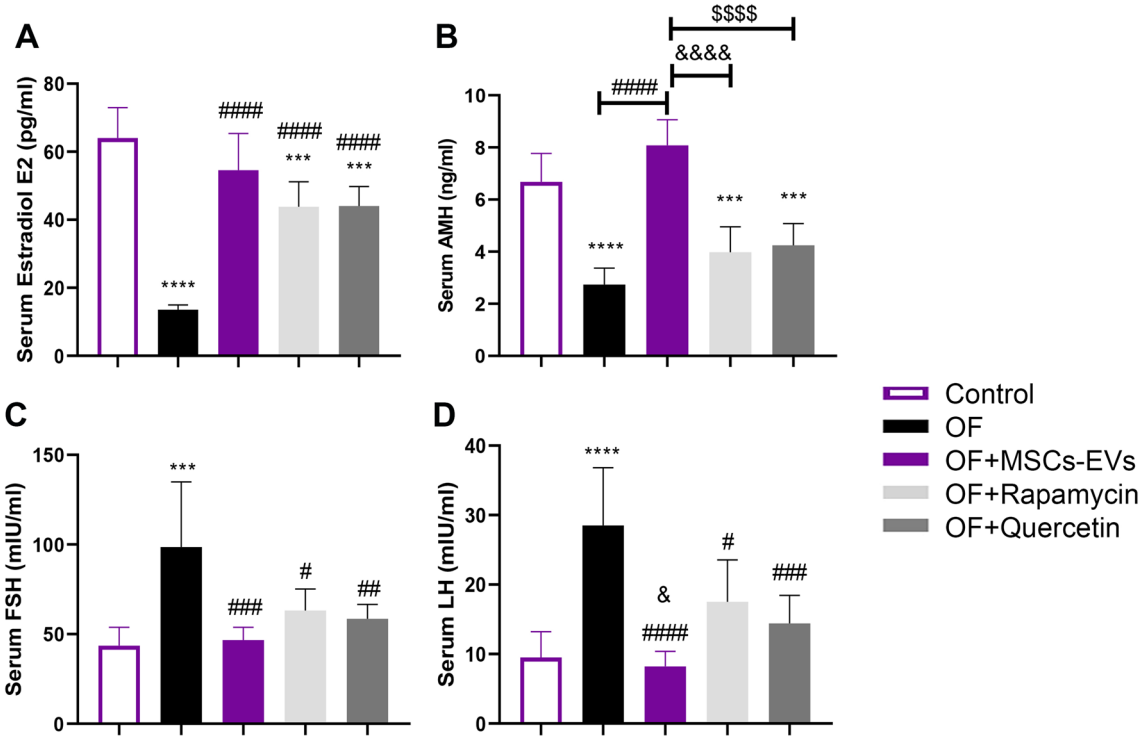

Fig. 4 Effect of MSCs-EVs, rapamycin, and quercetin on (**A**) serum Estradiol (E2), (**B**) serum anti-mullerian hormone (AMH), (**C**), serum follicle stimulating hormone (FSH), (**D**) serum luteinizing hormone (LH). Results are expressed as mean ± SEM. *** significant Vs control group at p<0.001, **** at p<0.0001, # significant vs. OF group at p<0.05, ## at p<0.01, ### at p<0.001, #### at p<0.0001, & significant vs. OF + Rapamycin group at p<0.05, &&&& at p<0.0001, $$$$ significant vs. OF + quercetin group at p<0.0001

($P<0.01$), Fig. 5B. At the protein level, ovarian FOXO3 level was markedly increased compared to the control group ($P<0.0001$). MSCs-EVs and rapamycin treatment markedly reduced ovarian FOXO3 levels compared to the OF group ($P<0.0001$, $P<0.001$), respectively, Fig. 5C, E. Further, chemotherapy was associated with increased phosphorylation of PI3K/AKT/mTOR axis in ovarian tissue as indicated by a significant increase in p-PI3K/PI3K ($P<0.0001$), p-AKT/AKT ($P<0.0001$), and p-mTOR/mTOR ($P<0.01$) when compared to the control group. MSCs-EVs, rapamycin, or quercetin significantly reduced p-PI3K/PI3K and p-AKT/AKT ($P<0.0001$) compared to the OF group. Regarding mTOR, MSCs-EVs, quercetin ($P<0.05$), and rapamycin ($P<0.001$) significantly reduced p-mTOR/mTOR compared to the OF group. However, no significant difference was observed between MSCs-EVs and the other treatment groups, Fig. 6.

Effect of MSCs-EVs on Micro-RNA modulating PI3K/AKT/mTOR axis

The expression levels of miRNA-200c ($P<0.01$), miRNA-122 ($P<0.05$), and miRNA-99a ($P<0.0001$) were significantly decreased in the OF group compared to the control group. MSCs-EVs administration resulted in a marked increase in expression levels of miRNA-200c, miRNA-122, and miRNA-99a ($P<0.0001$) compared to the OF group. Rapamycin and quercetin treatment showed no significant effect on miRNA-200c and miRNA-122 expression levels compared to the OF group. However, both treatments significantly increased miRNA-99a ($P<0.0001$) expression level compared to the OF group, Fig. 7.

Network analysis of biological pathways

The analysis of biological pathways affected by the PTEN and FOXO3 genes using FunRich software (Fig. 8A) revealed their significant involvement in several critical signaling networks. Most notably, the genes demonstrated complete (100%) participation in the mTOR signaling pathway and the class I PI3K signaling events, including those mediated by the Akt kinase. This highlights the central role of PTEN and FOXO3 in regulating these pivotal cascades. Furthermore, the genes exhibited 50% involvement in the PI3K/AKT activation pathway, the FOXO family signaling network, the p53 pathway, PI3 kinase-mediated AKT activation, and the PI-3 kinase cascade. All of these pathway alterations were statistically significant, with a P-value less than 0.05, underscoring the critical regulatory functions of PTEN and FOXO3 in cellular processes relevant to ovarian toxicity.

The molecular interaction network analysis (Fig. 8B) revealed the pivotal roles of the PTEN and FOXO3 genes

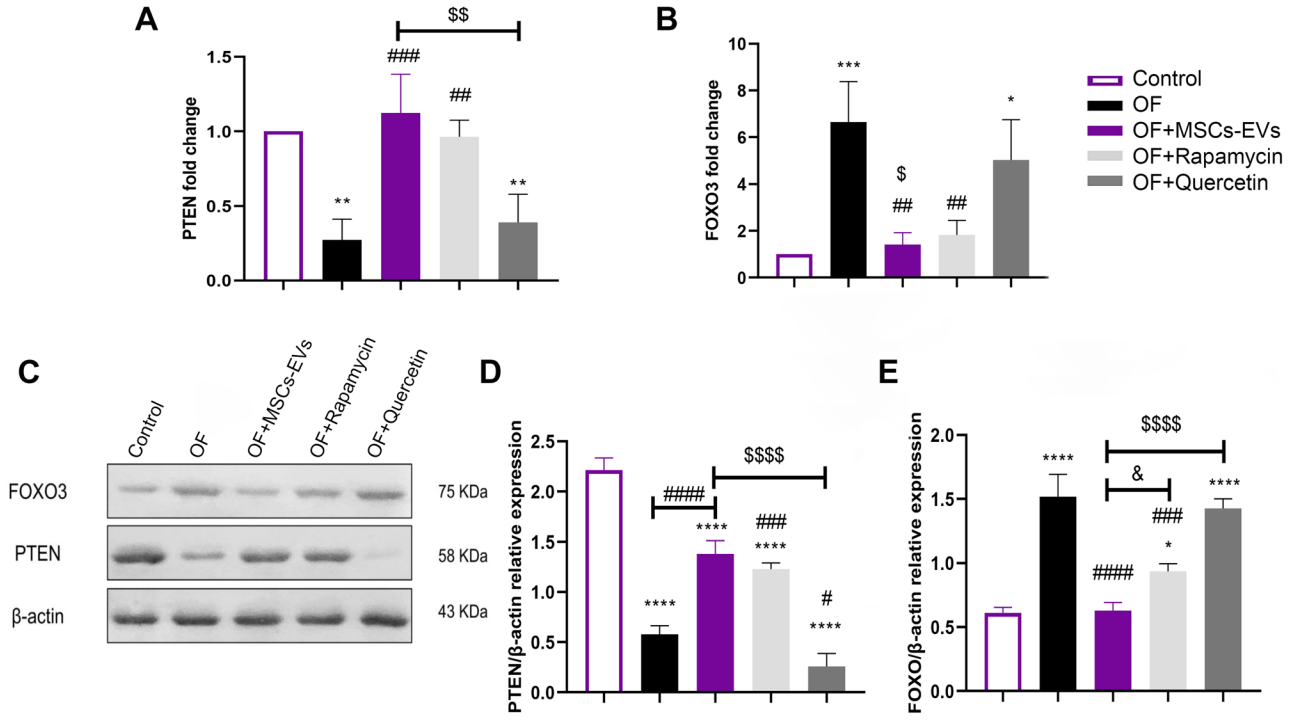

Fig. 5 Effect of MSCs-EVs, rapamycin, and quercetin on (**A**) relative gene expression of PTEN, (**B**) FOXO3, (**C**) Ovarian levels of PTEN and FOXO3 as detected by western blot analysis, (**D**, **E**) Intensity of immunoreactivity of selected proteins as quantified by densitometry. Results are expressed as mean ± SEM. *significant vs. Control group at p<0.05, ** at p<0.01, **** at p<0.0001, # significant vs. OF group at p<0.05, ## at p<0.01, ### at p<0.001, #### at p<0.0001. & significant vs. OF + Rapamycin group at p<0.05, $ significant vs. OF + quercetin group at p<0.05, $$ at p<0.01, $$$$ at p<0.0001

in regulating key signaling pathways associated with chemotherapy-induced ovarian toxicity. A prominent feature of the network was the centrality of PTEN and FOXO3 in modulating the mTOR signaling pathway. The statistically significant ($P<0.05$) interactions between these genes suggest that PTEN and FOXO3 are critical mediators of the apoptotic response to chemotherapeutic agents in ovarian cells.

The analysis of biological pathways affected by the miRNA-200c, miRNA-122, and miRNA-99 using FunRich software revealed several key findings (Fig. 8C). The Class I PI3K signaling events mediated by Akt, which play a crucial role in ovarian function, were found to contribute 33.3% to the overall pathway landscape. This emphasizes the significant impact these miRNAs have on this critical signaling axis. The mTOR signaling pathway was found to account for 33.3% of the affected biological pathways. The Class I PI3K signaling events, which are closely linked to the PI3K/AKT pathway, also showed a 33.3% contribution, further reinforcing the miRNAs' influence on key signaling cascades that are known to be dysregulated in chemotherapy-induced ovarian toxicity. Additionally, the analysis revealed the involvement of the FOXO family signaling (2.9%) and the PI3K/AKT activation (1.8%) pathways, both of which are closely associated with cellular stress response and apoptosis regulation. The statistical significance threshold of $P<0.05$ applied in this analysis underscores the robust nature of these findings, indicating that the observed pathway alterations are unlikely to have occurred by chance.

MSCs- EVs modulated cellular proliferation and apoptosis to mitigate OF

Examination of the immuno-stained sections for Ki67, BAX, and BCL2 provided insights into cellular proliferation and apoptosis, and their link to ovarian failure. Ki67 is a proliferation marker that indicates the presence of actively dividing cells. Examination of Ki67 immuno-stained sections of the control group revealed an intense nuclear immunoreaction in the granulosa cells of the developing follicles, Fig. 9a &b. Contrarily, a weak nuclear reaction was observed in the granulosa cells of the atretic follicles of the OF group following chemotherapy, Fig. 9c&d. In OF+MSCs-EVs group, administration of MSCs-EVs led to restoration of a moderate immunoreaction in the granulosa cells of the developing follicles, Fig. 9e&f. A mild and weak immunoreaction was observed in the granulosa cells of the follicles of OF groups receiving Rapamycin and quercetin respectively, Fig. 9h & j. Statistically, the Allred score for Ki67 immunoreactivity demonstrated a significant decrease ($P<0.0001$) in the OF group compared to the control

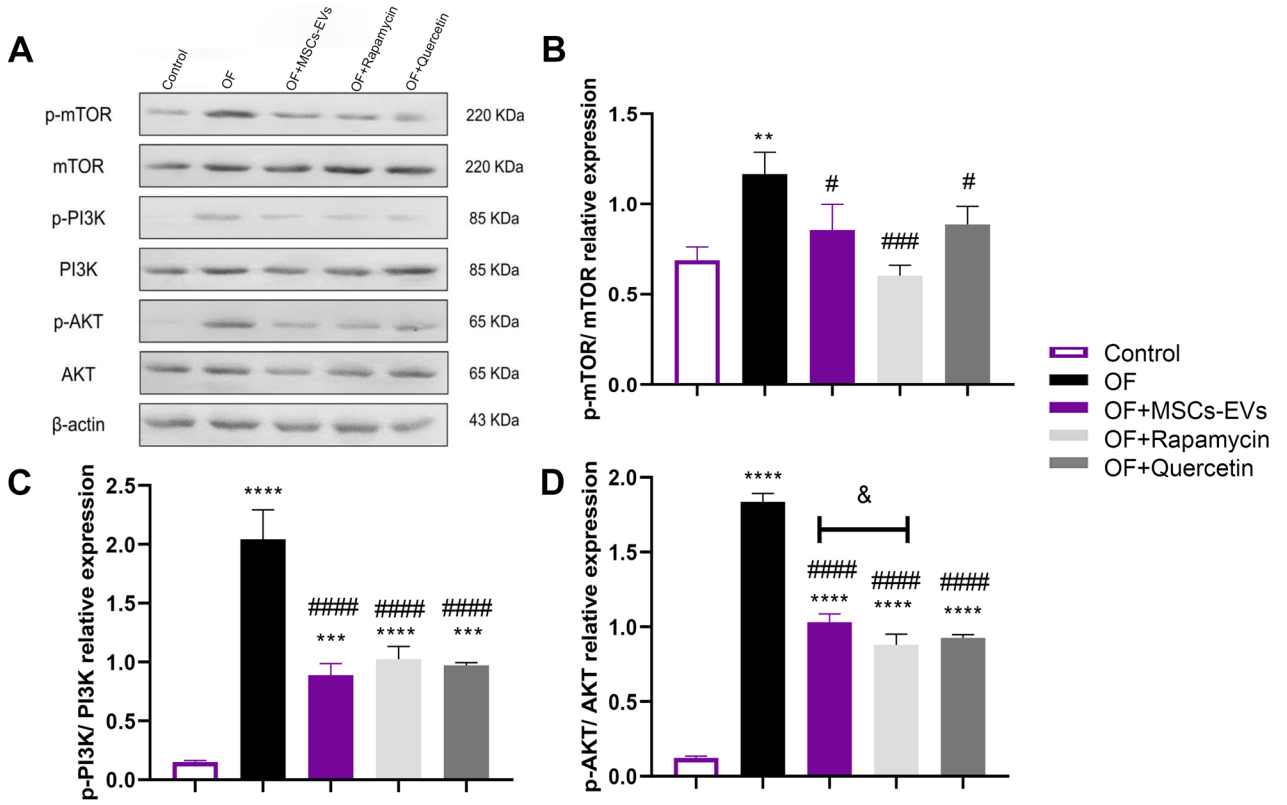

Fig. 6 Effect of MSCs-EVs, rapamycin, and quercetin on (**A**) phosphorylation of mTOR, PI3K, and AKT as detected by western blot analysis, (**B**-**D**) Intensity of immunoreactivity of selected proteins as quantified by densitometry. Results are expressed as mean ± SEM. **significant vs. Control group at p<0.01, **** at p<0.0001, # significant vs. OF group at p<0.05, ## at p<0.01, ### at p<0.001, #### at p<0.0001, & significant vs. OF + Rapamycin group at p<0.05

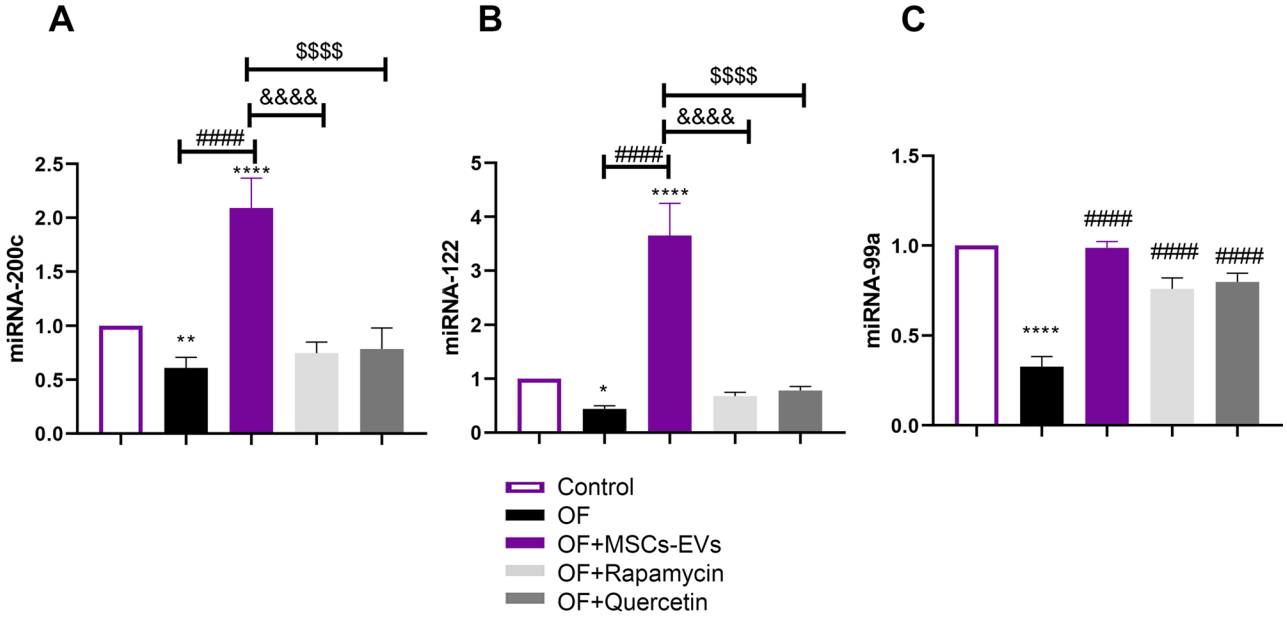

Fig. 7 Effect of MSCs-EVs, rapamycin, and quercetin on (**A**) miRNA-200c (**B**) miRNA-122 (**C**) miRNA-99a relative expression in ovarian tissues. Results are expressed as mean ± SEM. *significant vs. Control group at p<0.05, ** at p<0.01, **** at p<0.0001, #### significant vs. OF group at p<0.0001. &&&& significant vs. OF + Rapamycin group at p<0.0001, $$$$ significant vs. OF + quercetin group at p<0.0001

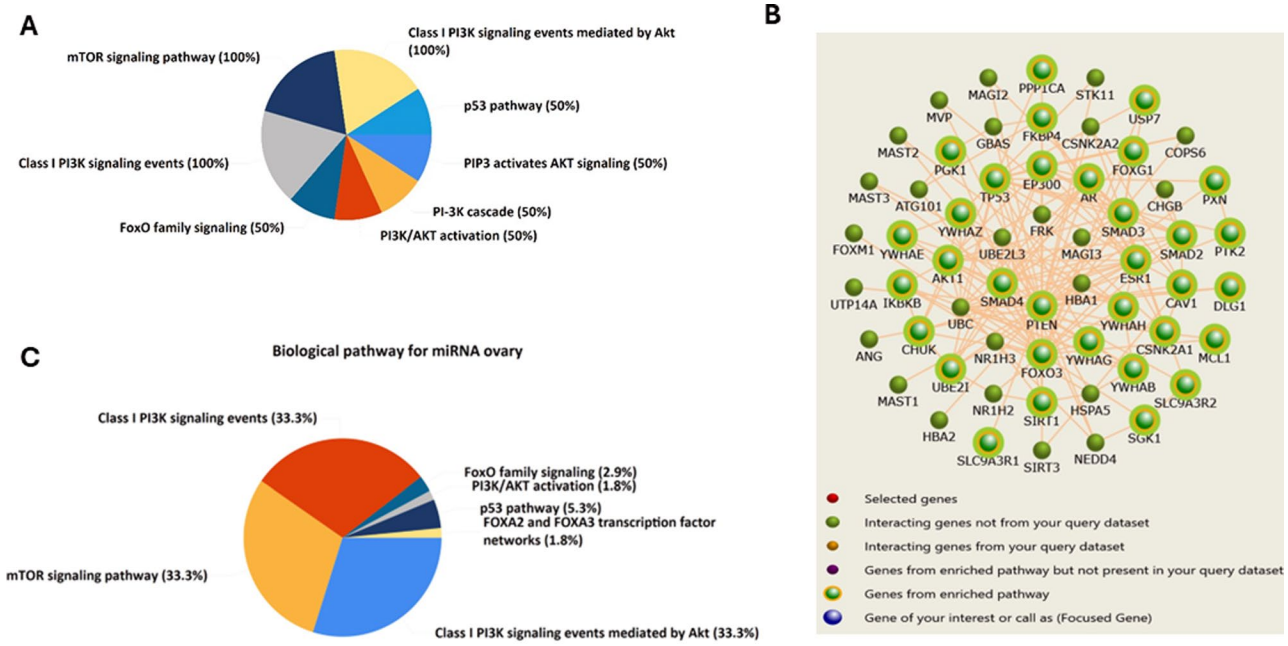

Fig. 8 **A**) Analysis of the biological pathways affected by PTEN, FOXO3 genes using FunRich software. $P<0.05$ indicates a statistically significant difference. **B**) Molecular interaction network of PTEN, FOXO3 genes determined using FunRich software. $P<0.05$ was considered to indicate a statistically significant difference. **C**) Biological pathways affected by miR-200c, miR-122, and miR-99 according to FunRich software. $P<0.05$ indicates a statistically significant difference

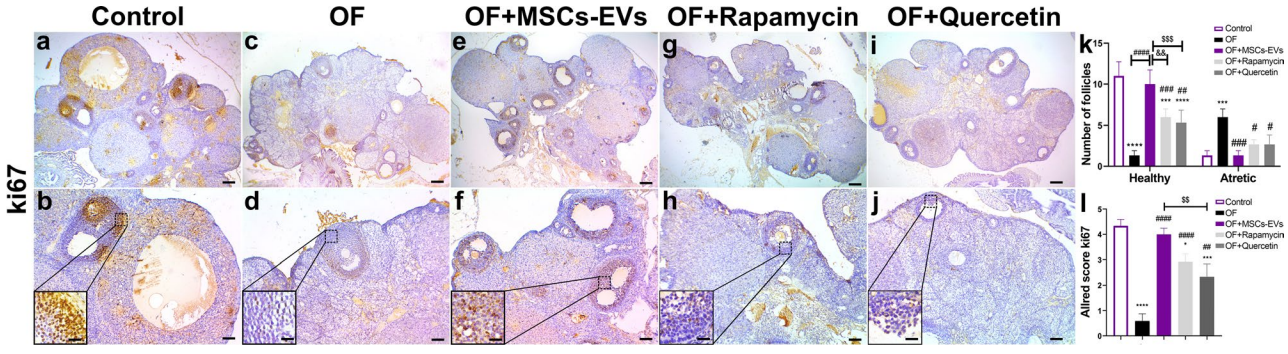

Fig. 9 Representative photomicrographs of Ki67 immuno-stained sections. **a, b**) Group I: intense, **c, d**) Group II: weak, **e, f**) Group III: moderate, **g, h**) Group IV: mild, **i, j**) Group V: weak, nuclear immunoreaction in the granulosa cells of the follicles. **k**): Histogram demonstrating healthy and atretic follicles. **l**) Allred score for Ki67 immuno reactivity, * significant vs. Control group at p<0.05, *** at p<0.001, ## significant vs. OF group at p<0.01, #### at p<0.0001. $$ significant vs. OF + Quercetin group at p<0.01

group. MSCs-EVs and Rapamycin treatment significantly increased Ki67 Allred score when compared to the OF group ($P<0.0001$). A less significant increase in Ki67 Allred score was observed in the quercetin-treated group compared to the OF group ($P<0.01$), Fig. 9l.

BAX is an apoptosis marker that indicates the presence of apoptotic cells. In the control group, a weak immunoreaction was observed in a few granulosa cells of the follicles, suggesting a low level of apoptosis, Fig. 10a &b. Following chemotherapy in the OF group, an intense immunoreaction was observed in many granulosa cells of atretic follicles, indicating increased apoptotic activity, Fig. 10c&d. However, in the OF+MSCs-EVs group, the immunoreactivity was similar to the control group, suggesting inhibition of apoptosis, Fig. 10e&f. In the OF+rapamycin group, a moderate immunoreaction was detected in a few cells, indicating a partial reduction in apoptotic activity, Fig. 10g&h. In the OF+quercetin group, an intense immunoreaction was observed in numerous granulosa cells, suggesting an increase in apoptotic activity, Fig. 10i&j. Statistically, the Allred score for BAX immunoreactivity demonstrated a significant increase in BAX Allred score in the OF group compared to the control group ($P<0.0001$). Treatment with MSCs-EVs, Rapamycin ($P<0.0001$), and quercetin ($P<0.01$)

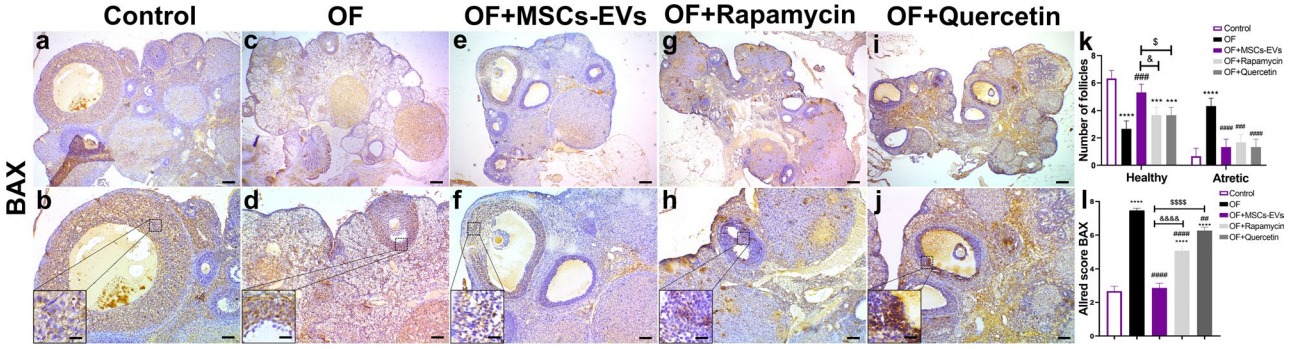

Fig. 10 Representative photomicrographs of BAX immuno-stained sections. **a, b**) Group I: weak (curved arrow), **c, d**) Group II: intense, **e, f**) Group III: weak, **g, h**) Group IV: moderate, **i, j**) Group V: intense nuclear immunoreaction in the granulosa cells of the follicles. **k**) Histogram demonstrating healthy and atretic follicles. **l**) Allred score for BAX immunoreactivity, ****significant vs. Control group at p<0.0001, ## significant vs. OF group at p<0.01, #### at p<0.0001. &&&& significant vs. OF + Rapamycin group at p<0.0001, $$$$ significant vs. OF + Quercetin group at p<0.0001

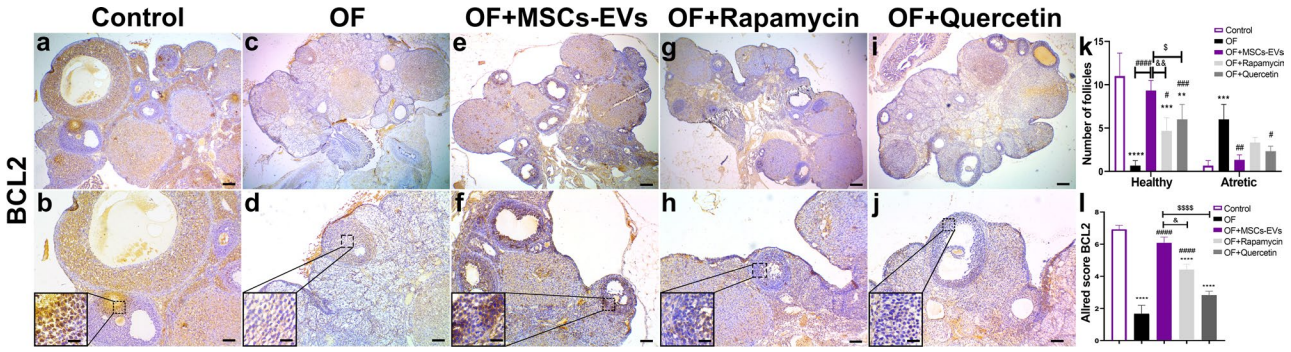

Fig. 11 Representative photomicrographs of BCL2 immuno-stained sections. **a, b**) Group I: intense, **c, d**) Group II: weak, **e, f**) Group III: intense, **g, h** and **i, j**) Group IV & V: moderate and weak immunoreaction in the numerous and few granulosa cells respectively. **k**) Histogram demonstrating healthy and atretic follicles. **l**) Allred score for BCL2 immunoreactivity, **** significant vs. Control group at p<0.0001, #### significant vs. OF group at p<0.0001, & significant vs. OF + Rapamycin group at p<0.05, $$$$ significant vs. OF + Quercetin group at p<0.0001

markedly reduced Allred score compared to the OF group, Fig. 10l.

BCL2 is an anti-apoptotic marker that indicates the presence of cells protected against apoptosis. In the control group, an intense immunoreaction was observed in the granulosa cells of the follicles, indicating high levels of anti-apoptotic activity, Fig. 11a &b. However, following chemotherapy in the OF group, a weak immunoreaction was observed in the granulosa cells of atretic follicles, suggesting reduced anti-apoptotic activity, Fig. 11c&d. In the OF+MSCs-EVs group, the immunoreactivity was similar to the control group, indicating restoration of anti-apoptotic activity, Fig. 11e&f. In the OF+rapamycin group, a moderate immunoreaction was detected in numerous granulosa cells, suggesting partial restoration of anti-apoptotic activity, Fig. 11g&h. In the OF+quercetin group, a weak immunoreaction was observed in fewer granulosa cells, indicating a partial increase in anti-apoptotic activity, Fig. 11i&j. Statistical analysis of the BCL2 Allred score revealed a significant decrease ($P<0.0001$) in BCL2 Allred score in the OF group compared to the control group. Treatment with MSCs-EVs and Rapamycin markedly restored Allred score ($P<0.0001$) compared to the OF group. Non-significant difference in BCL2 Allred score was observed in the quercetin-treated group when compared to the OF group, Fig. 11.

Discussion

Several studies have investigated the link between chemotherapy and OF and have highlighted chemotherapy's detrimental impact on the ovaries. Chemotherapy not only targets tumor cells but also induces apoptosis in normal tissues, including the ovaries [2]. Ovarian cultures and animal models have provided evidence of the damaging effects of chemotherapy on the ovaries [32]. Insufficient activation of DNA repair mechanisms can lead to cellular apoptosis [33], which aligns with the findings of the current study. The OF group exhibited a significant decrease in serum E2 and AMH levels, accompanied by a notable increase in FSH and LH levels. AMH is produced by ovarian follicles and used as an indicator of ovarian reserve [34]. It contributes to the maintenance of the ovarian reserve by regulating oocyte maturation and preventing follicular development [35]. Decreased AMH and E2 levels and increased FSH and LH levels are linked with ovarian insufficiency [36]. Chemotherapy has been

reported to affect ovarian steroidogenesis, the process by which somatic cells in the ovary produce and secrete female sex steroidal hormones. This can explain the hormonal alterations observed in the OF group [37]. Also, chemotherapy causes mature follicles to directly undergo apoptosis, which perturbs the negative regulatory feedback loop on the recruitment of primordial follicles and ultimately results in the recruitment of primordial follicles prematurely. In the present study, histological examination of ovarian sections revealed an increase in atretic follicles. Immunostaining demonstrated a significant increase in BAX-positive apoptotic granulosa cells, a reduction in Ki67-positive proliferating granulosa cells, and a decrease in antiapoptotic BCL2-positive granulosa cells. These results collectively indicate that chemotherapy induces an OF phenotype.

The specific mechanisms underlying chemotherapy-induced ovarian damage are still not fully understood. According to recent studies, chemotherapy-induced OF may be exacerbated by the "burn-out effect" or direct DNA damage to the follicle reserve [38]. Chemotherapy can interfere with the PI3K/AKT signaling pathway, which is responsible for follicle quiescence, leading to the overactivation of primordial follicles and depletion of the follicle reserve [39]. Furthermore, as follicles grow and develop, granulosa cells proliferate extensively and become increasingly susceptible to the deleterious effects of chemotherapy. This may cause a large number of growing follicles to undergo apoptosis, which would decrease the secretion of inhibitory factors and indirectly recruit primordial follicles into the growing pool [40]. Moreover, FOXO3 represents another downstream effector of PI3K/AKT pathway. Modulation of PI3K/AKT/FOXO3a signaling promoted follicle growth, restored ovarian function, and suppressed oxidative stress in chemotherapy-induced OF [41]. In line, the OF group of the current study demonstrated an increase in phosphorylation of signaling pathway proteins PI3K, AKT, and mTOR, an increase in gene expression and protein of FOXO3 concomitant with a decrease in gene expression and protein of PTEN, a negative regulator of PI3K/AKT signaling, suggesting that chemotherapy-induced overactivation of primordial follicles may be mediated by triggering mTOR signaling.

The mammalian target of rapamycin (mTOR) signaling, a key downstream element of the PI3K/AKT pathway, plays an essential role in the regulation of the cell cycle [14]. Besides regulating cell survival, growth, proliferation, and migration, mTOR also orchestrates gene transcription, protein synthesis, and cell autophagy [42]. Interestingly, rapamycin, an mTOR inhibitor, binds to the cytosolic protein FKBP12 to form a complex. The complex then binds with the FKBP12-rapamycin-binding domain of mTOR, thereby inhibiting mTOR's activity [43]. Notably, lack of PTEN in mouse oocytes, or specific deletion of tsc1 and tsc2 resulted in premature activation of primordial follicles in mouse ovaries leading to follicular depletion in early adulthood [44]. This suggests that hyperactivation of mTORC1 signaling can accelerate primordial follicle activation, and mTORC1's inhibitor, rapamycin, can inhibit primordial follicle development and conserve the follicular pool by suppressing this signaling pathway. Indeed, rapamycin has been found to partially counter the stimulatory effect of SD208, a transforming growth factor beta receptor I kinase inhibitor, on oocyte growth, thereby reducing the number of growing follicles [45].

Using chemotherapy and rapamycin simultaneously in this study significantly reduced the ratio of mature follicles to primordial follicles in rat ovaries, implying inhibition of primordial follicle recruitment in the OF and rapamycin-treated group. Consistently, rapamycin has been previously reported to suppress the recruitment of primordial follicles in mice ovaries by blocking mTORC1 [46]. On the other hand, similar results were observed in the OF group with quercetin, a PI3K inhibitor. Quercetin treatment reduced the phosphorylation levels of PI3K, Akt, and mTOR. These findings suggest quercetin may block chemotherapy-induced primordial to primary follicle transformation by inhibiting the PI3K signaling pathway. These outcomes are in line with earlier research that documented quercetin's protective effectiveness against chemotherapy-induced ovarian insufficiency [26, 47].

In the present study, MSCs-EVs administration to chemotherapy-treated rats decreased the number of atretic follicles. It increased the number of normal follicles while almost normalizing hormonal levels of AMH, FSH, and E2. Further, MSCs-EVs restored ovarian PTEN expression, suppressed PI3K, AKT, and mTOR phosphorylation, and FOXO3 expression, leading to apoptosis suppression and triggering granulosa cell proliferation. These results were comparable to those obtained from the groups treated with rapamycin on quercetin. The results from this molecular interaction network analysis emphasize the pivotal regulatory functions of PTEN and FOXO3 in orchestrating the complex signaling events that govern ovarian cell survival and response to chemotherapeutic agents. These findings provide valuable insights into the potential mechanisms by which targeting these genes and their associated pathways, such as mTOR and PI3K/AKT, could mitigate the detrimental effects of chemotherapy on ovarian function.

The ability of MSCs-EVs to attenuate the apoptosis of granulosa cells and atresia of follicles was further confirmed by assessing the immunoexpression of Ki67 which showed increased immunostaining in granulosa cells of antral follicles in the MSCs-EVs group. Additionally, Bcl-2 immunostaining was significantly increased and

BAX immunostaining was significantly reduced, indicating decreased apoptosis in granulosa cells. By forming a dimer with BAX, Bcl-2 exerts an anti-apoptotic effect. These effects contribute to the preservation of ovarian function and the prevention of ovarian failure. Indeed, increased ovarian Bcl-2 expression antagonized the effect of Bax, leading to the inhibition of apoptosis of granulosa cells [48].

Ovarian stroma plays a crucial part in follicular dynamics by actively participating in paracrine signalling in addition to providing structural support [49]. The present study findings indicated increased BAX immune-expression in the stroma of treatment groups, reflecting its crucial role in adaptive response to chemotherapy. The elevated BAX levels in the treatment groups suggest that the stroma engages in a regulatory mechanism balancing apoptotic and anti-apoptotic signals. While BAX is typically associated with pro-apoptotic activity, its increased expression in this context may represent an active modulation of the apoptotic response, facilitating ovarian function preservation. Moreover, the overall significant decrease in pro-apoptotic signaling and the increase in anti-apoptotic Bcl-2 expression compared to OF group imply that the stroma effectively counters chemotherapy effects. By maintaining a favourable environment through paracrine signaling, the stroma supports granulosa cell survival and enhances overall ovarian recovery. This dual role underscores the importance of the stroma in ovarian physiology and its potential as a therapeutic target in reproductive medicine.

Stem cell-derived EVs present considerable potential as a cell-free treatment strategy to improve ovarian function and fertility [50]. The use of MSC-Exos to treat infertility and ovarian aging is being investigated. these treatments provide promising beneficial effects in cases of reduced ovarian reserve, or POI, by attempting to repair damaged tissues and enhance ovarian function [51]. Specifically, Recent studies highlight key benefits of MSCs-EVs in treating chemotherapy-induced POF. Zhang et al. reported that MSCs-derived exosomes promote the proliferation of ovarian granulosa cells and preserve fertility in chemotherapy-induced POI model [52]. Zhou et al. indicated that MSCs-derived exosomes mitigate ferroptosis and protect against POI via the Nrf2/GPX4 signalling pathway [53].

The therapeutic efficacy of EVs derived from MSCs can be elucidated through the release of various MSCs-EVs microRNAs (EVs-miRNAs) [54]. These microRNAs exhibit the potential to modulate key signaling pathways in ovarian tissues. Herein, results demonstrated an increase in the levels of miR-200c, miR-122, and miR-99a in MSCs-EVs treated group, suggesting that the cargo of released microRNAs from MSC-EVs exerts inhibitory effects on the PI3K/AKT/mTOR signaling pathway by targeting PI3K (miR-200c) [55], AKT (miR-122) [56], and mTOR (miR-99a) [57]. These findings were futher reinforced by results of netwotk analysis, providing valuable insights into the molecular mechanisms underlying the therapeutic potential of MSC- EVs in ovarian failure. However, further investigation is required to determine whether this effect is de novo from the ovarian tissues or MSCs-EVs.

Conclusion

The present study demonstrated that MSCs-derived EVs could be beneficial in halting chemotherapy-induced ovarian insufficiency. Co-treatment with EVs preserves primordial follicles, enhances proliferation, and reduces apoptosis of granulosa cells in ovarian tissues. Targeting PI3K/AKT/mTOR by miRNA could be in part a possible mechanism. However, further investigations are needed to prove that miRNAs in EVs are the major driver of the observed effects.

Acknowledgements

The authors extend their appreciation to the Deanship of Scientific Research at the University of Tabuk for funding this work through research number S-1443-0065.

Author contributions

N.M.E. and N.E.: Conceptualization and Formal Analysis; O.A.M.B., A.A.D. and N.E.: Methodology and prepartaion of the figures; M.S.A., K.P., H.A. and O.A.A.: Investigation, Validation and Visualization; Z.M.M., A.S.F. and A.A.S.: Resourses; N.M.E., O.A.M.B., A.A.D. and N.E: Writing – original draft. All authors reviewed the manuscript.

Funding

The authors extend their appreciation to the Deanship of Research and Graduate Studies at University of Tabuk for funding this work through Research number S-1443-0065.

Data availability

All data supporting the findings of this study are available on request.

Declarations

Institutional review board statement

The experimental procedure was conducted in compliance with the National Institutes of Health's Guide for the Care and Use of Laboratory Animals (NIH publication No. 85–23, revised 2011) and carried out following the institutional review board for animal experiments of the Faculty of Medicine, Benha University, Egypt (BUFVTM 07-07-22).

Competing interests

The authors declare no competing interests.

Author details

[1]Department of Pharmaceutical Chemistry, Faculty of Pharmacy, University of Tabuk, Tabuk, Saudi Arabia
[2]Department of Pharmacology & Toxicology, Faculty of Pharmacy, University of Tabuk, Tabuk, Saudi Arabia
[3]Department of Pharmacy Practice, Faculty of Pharmacy, University of Tabuk, Tabuk, Saudi Arabia
[4]Department of Medical Laboratory Technology, Faculty of Applied Medical Sciences, University of Tabuk, Tabuk 71491, Saudi Arabia
[5]Department of Genetics and Genetic Engineering, Faculty of Agriculture, Benha University, Benha, Egypt
[6]Department of Medical Histology and Cell Biology, Faculty of Medicine, Zagazig University, Zagazig 44519, Egypt

[7]PharmD Program, Faculty of Pharmacy, University of Tabuk, Tabuk, Saudi Arabia
[8]Department of Clinical Pathology, Faculty of Veterinary Medicine, Benha University, Moshtohor, Toukh, Qalyubia 13736, Egypt
[9]Surgery, Anesthesiology and Radiology Department, Faculty of Veterinary Medicine, Cairo University, Cairo, Egypt
[10]Department of Medical Histology and Cell Biology Faculty of Medicine, Benha University, Benha, Egypt
[11]Stem Cell Unit, Faculty of Medicine, Benha University, Benha, Egypt
[12]Faculty of Medicine, Benha National University, Al Obour City, Egypt
[13]Cell and Tissue Engineering, School of Pharmacy and Bioengineering, Keele University, Keele, UK

Received: 7 August 2024 / Accepted: 24 October 2024
Published online: 11 November 2024

References

1. Mauri D, Gazouli I, Zarkavelis G, Papadaki A, Mavroeidis L, Gkoura S, et al. Chemother Assoc Ovarian Fail Front Endocrinol (Lausanne). 2020;11:572388.
2. Spears N, Lopes F, Stefansdottir A, Rossi V, De Felici M, Anderson RA, et al. Ovarian damage from chemotherapy and current approaches to its protection. Hum Reprod Update. 2019;25(6):673–93.
3. Donnez J, Dolmans MM. Fertility preservation in women. N Engl J Med. 2017;377(17):1657–65.
4. Donnez J, Martinez-Madrid B, Jadoul P, Van Langendonckt A, Demylle D, Dolmans MM. Ovarian tissue cryopreservation and transplantation: a review. Hum Reprod Update. 2006;12(5):519–35.
5. Del Castillo LM, Buigues A, Rossi V, Soriano MJ, Martinez J, De Felici M, et al. The cyto-protective effects of LH on ovarian reserve and female fertility during exposure to gonadotoxic alkylating agents in an adult mouse model. Hum Reprod. 2021;36(9):2514–28.
6. Sonigo C, Beau I, Binart N, Grynberg M. The impact of Chemotherapy on the ovaries: molecular aspects and the Prevention of ovarian damage. Int J Mol Sci. 2019;20(21):E5342.
7. Aljaser F. Preservation of fertility in female: indications, available options, and current status in Saudi Arabia. Semin Oncol. 2020;47(6):390–7.
8. Sonigo C, Beau I, Grynberg M, Binart N. AMH prevents primordial ovarian follicle loss and fertility alteration in cyclophosphamide-treated mice. FASEB J. 2019;33(1):1278–87.
9. Monniaux D, Clément F, Dalbiès-Tran R, Estienne A, Fabre S, Mansanet C, et al. The ovarian reserve of primordial follicles and the dynamic reserve of antral growing follicles: what is the link? Biol Reprod. 2014;90(4):85.
10. Adhikari D, Liu K. Molecular mechanisms underlying the activation of mammalian primordial follicles. Endocr Rev. 2009;30(5):438–64.
11. Shah JS, Sabouni R, Cayton Vaught KC, Owen CM, Albertini DF, Segars JH. Biomechanics and mechanical signaling in the ovary: a systematic review. J Assist Reprod Genet. 2018;35(7):1135–48.
12. Hsueh AJW, Kawamura K, Cheng Y, Fauser BCJM. Intraovarian Control of Early Folliculogenesis. Endocr Rev. 2015;36(1):1–24.
13. Zheng W, Nagaraju G, Liu Z, Liu K. Functional roles of the phosphatidylinositol 3-kinases (PI3Ks) signaling in the mammalian ovary. Mol Cell Endocrinol. 2012;356(1–2):24–30.
14. Goldman KN, Chenette D, Arju R, Duncan FE, Keefe DL, Grifo JA, et al. mTORC1/2 inhibition preserves ovarian function and fertility during genotoxic chemotherapy. Proc Natl Acad Sci U S A. 2017;114(12):3186–91.
15. Zhou L, Xie Y, Li S, Liang Y, Qiu Q, Lin H, et al. Rapamycin prevents cyclophosphamide-induced over-activation of primordial follicle pool through PI3K/Akt/mTOR signaling pathway in vivo. J Ovarian Res. 2017;10(1):56.
16. György B, Szabó TG, Pásztói M, Pál Z, Misják P, Aradi B, et al. Membrane vesicles, current state-of-the-art: emerging role of extracellular vesicles. Cell Mol Life Sci. 2011;68(16):2667–88.
17. Bidarimath M, Khalaj K, Kridli RT, Kan FWK, Koti M, Tayade C. Extracellular vesicle mediated intercellular communication at the porcine maternal-fetal interface: a new paradigm for conceptus-endometrial cross-talk. Sci Rep. 2017;7:40476.
18. Huang-Doran I, Zhang CY, Vidal-Puig A. Extracellular vesicles: Novel mediators of Cell Communication in metabolic disease. Trends Endocrinol Metab. 2017;28(1):3–18.
19. Li N, Zhao L, Geng X, Liu J, Zhang X, Hu Y, et al. Stimulation by exosomes from hypoxia-preconditioned hair follicle mesenchymal stem cells facilitates mitophagy by inhibiting the PI3K/AKT/mTOR signaling pathway to alleviate ulcerative colitis. Theranostics. 2024;14(11):4278–96.
20. Zheng T, Li S, Zhang T, Fu W, Liu S, He Y, et al. Exosome-shuttled mir-150-5p from LPS-preconditioned mesenchymal stem cells down-regulate PI3K/Akt/mTOR pathway via Irs1 to enhance M2 macrophage polarization and confer protection against sepsis. Front Immunol. 2024;15:1397722.
21. Liu C, Khairullina L, Qin Y, Zhang Y, Xiao Z. Adipose stem cell exosomes promote mitochondrial autophagy through the PI3K/AKT/mTOR pathway to alleviate keloids. Stem Cell Res Ther. 2024;15(1):305.
22. Ebrahim N, Al Saihati HA, Alali Z, Aleniz FQ, Mahmoud SYM, Badr OA, et al. Exploring the molecular mechanisms of MSC-derived exosomes in Alzheimer's disease: Autophagy, insulin and the PI3K/Akt/mTOR signaling pathway. Biomed Pharmacother. 2024;176:116836.
23. Huang TL, Jiang WJ, Zhou Z, Shi TF, Yu M, Yu M, et al. Quercetin attenuates cisplatin-induced mitochondrial apoptosis via PI3K/Akt mediated inhibition of oxidative stress in pericytes and improves the blood labyrinth barrier permeability. Chem Biol Interact. 2024;393:110939.
24. Ebrahim N, Ahmed IA, Hussien NI, Dessouky AA, Farid AS, Elshazly AM, et al. Mesenchymal stem cell-derived exosomes ameliorated diabetic nephropathy by autophagy induction through the mTOR signaling pathway. Cells. 2018;7(12):226.
25. Al Saihati HA, Badr OA, Dessouky AA, Mostafa O, Samir Farid A, Aborayah NH, et al. Exploring the cytoprotective role of mesenchymal stem cell-derived exosomes in chronic liver fibrosis: insights into the Nrf2/Keap1/p62 signaling pathway. Int Immunopharmacol. 2024;141:112934.
26. Li J, Long H, Cong Y, Gao H, Lyu Q, Yu S, et al. Quercetin prevents primordial follicle loss via suppression of PI3K/Akt/Foxo3a pathway activation in cyclophosphamide-treated mice. Reprod Biol Endocrinol. 2021;19(1):63.
27. Livak KJ, Schmittgen TD. Analysis of relative gene expression data using real-time quantitative PCR and the 2 – ΔΔCT method. Methods. 2001;25(4):402–8.
28. Suvarna KS, Layton C, Bancroft JD, editors. Theory and practice of histological techniques. 7 ed. Edinburgh: Elsevier Churchill Livingston; 2013. p. 637.
29. Fedchenko N, Reifenrath J. Different approaches for interpretation and reporting of immunohistochemistry analysis results in the bone tissue - a review. Diagn Pathol. 2014;9:221.
30. Bankhead P, Loughrey MB, Fernández JA, Dombrowski Y, McArt DG, Dunne PD, et al. QuPath: open source software for digital pathology image analysis. Sci Rep. 2017;7(1):16878.
31. Li Y, Cheng Q, Hu G, Deng T, Wang Q, Zhou J, et al. Extracellular vesicles in mesenchymal stromal cells: a novel therapeutic strategy for stroke. Exp Ther Med. 2018;15(5):4067–79.
32. Sonigo C, Beau I, Binart N, Grynberg M. The impact of Chemotherapy on the ovaries: molecular aspects and the Prevention of ovarian damage. Int J Mol Sci. 2019;20(21):5342.
33. Chatterjee N, Walker GC. Mechanisms of DNA damage, repair, and mutagenesis. Environ Mol Mutagen. 2017;58(5):235–63.
34. Kozlowski IF, Carneiro MC, da Rosa VB, Schuffner A. Correlation between anti-Müllerian hormone, age, and number of oocytes: a retrospective study in a Brazilian in vitro fertilization center. JBRA Assist Reprod. 2022;26(2):214–21.
35. Xu H, Zhang M, Zhang H, Alpadi K, Wang L, Li R, et al. Clinical applications of serum Anti-Müllerian hormone measurements in both males and females: an update. Innov (Camb). 2021;2(1):100091.
36. Jiao X, Meng T, Zhai Y, Zhao L, Luo W, Liu P, et al. Ovarian Reserve markers in premature ovarian insufficiency: within different clinical stages and different etiologies. Front Endocrinol (Lausanne). 2021;12:601752.
37. Jamnongjit M, Hammes SR. Ovarian steroids: the good, the bad, and the signals that raise them. Cell Cycle. 2006;5(11):1178–83.
38. Szymanska KJ, Tan X, Oktay K. Unraveling the mechanisms of chemotherapy-induced damage to human primordial follicle reserve: road to developing therapeutics for fertility preservation and reversing ovarian aging. Mol Hum Reprod. 2020;26(8):553–66.
39. Kashi O, Meirow D. Overactivation or apoptosis: which mechanisms affect Chemotherapy-Induced Ovarian Reserve Depletion? Int J Mol Sci. 2023;24(22):16291.
40. Yang Y, Tang X, Yao T, Zhang Y, Zhong Y, Wu S, et al. Metformin protects ovarian granulosa cells in chemotherapy-induced premature ovarian failure mice through AMPK/PPAR-γ/SIRT1 pathway. Sci Rep. 2024;14(1):1447.
41. Su C, Zhang R, Zhang X, Lv M, Liu X, Ao K, et al. Dingkun Pill modulate ovarian function in chemotherapy-induced premature ovarian insufficiency mice by regulating PTEN/PI3K/AKT/FOXO3a signaling pathway. J Ethnopharmacol. 2023;315:116703.

42. Yu JJ, Goncharova EA. mTOR Signaling Network in Cell Biology and Human Disease. IJMS. 2022;23(24):16142.
43. Hu L, Chen F, Wu C, Wang J, Chen SS, Li XR, et al. Rapamycin recruits SIRT2 for FKBP12 deacetylation during mTOR activity modulation in innate immunity. iScience. 2021;24(11):103177.
44. Zhang T, He M, Zhang J, Tong Y, Chen T, Wang C, et al. Mechanisms of primordial follicle activation and new pregnancy opportunity for premature ovarian failure patients. Front Physiol. 2023;14:1113684.
45. Bai X, Wang S. Signaling pathway intervention in premature ovarian failure. Front Med (Lausanne). 2022;9:999440.
46. Chen X, Tang Z, Guan H, Xia H, Gu C, Xu Y, et al. Rapamycin maintains the primordial follicle pool and protects ovarian reserve against cyclophosphamide-induced damage. J Reprod Dev. 2022;68(4):287–94.
47. Zubčić K, Radovanović V, Vlainić J, Hof PR, Oršolić N, Šimić G, et al. PI3K/Akt and ERK1/2 signalling are involved in quercetin-mediated neuroprotection against Copper-Induced Injury. Oxid Med Cell Longev. 2020;2020:9834742.
48. Chi XX, Zhang T, Chu XL, Zhen JL, Zhang DJ. The regulatory effect of Genistein on granulosa cell in ovary of rat with PCOS through Bcl-2 and Bax signaling pathways. J Veterinary Med Sci. 2018;80(8):1348–55.
49. Kinnear HM, Tomaszewski CE, Chang AL, Moravek MB, Xu M, Padmanabhan V, et al. The ovarian stroma as a new frontier. Reproduction. 2020;160(3):R25–39.
50. Luo Y, Chen J, Ning J, Sun Y, Chai Y, Xiao F, et al. Stem cell-derived extracellular vesicles in premature ovarian failure: an up-to-date meta-analysis of animal studies. J Ovarian Res. 2024;17(1):182.
51. Cui X, Jing X. Stem cell-based therapeutic potential in female ovarian aging and infertility. J Ovarian Res. 2024;17(1):171.
52. Zhang L, Ma Y, Xie X, Du C, Zhang Y, Qin S, et al. Human pluripotent stem cell-mesenchymal stem cell-derived exosomes promote ovarian Granulosa Cell Proliferation and Attenuate Cell apoptosis Induced by Cyclophosphamide in a POI-like mouse model. Molecules. 2023;28(5):2112.
53. Zhou Y, Huang J, Zeng L, Yang Q, Bai F, Mai Q, et al. Human mesenchymal stem cells derived exosomes improve ovarian function in chemotherapy-induced premature ovarian insufficiency mice by inhibiting ferroptosis through Nrf2/GPX4 pathway. J Ovarian Res. 2024;17(1):80.
54. Kou M, Huang L, Yang J, Chiang Z, Chen S, Liu J, et al. Mesenchymal stem cell-derived extracellular vesicles for immunomodulation and regeneration: a next generation therapeutic tool? Cell Death Dis. 2022;13(7):580.
55. Zhou G, Zhang F, Guo Y, Huang J, Xie Y, Yue S, et al. miR-200c enhances sensitivity of drug-resistant non-small cell lung cancer to gefitinib by suppression of PI3K/Akt signaling pathway and inhibites cell migration via targeting ZEB1. Biomed Pharmacother. 2017;85:113–9.
56. Li KW, Wang SH, Wei X, Hou YZ, Li ZH. Mechanism of mir-122-5p regulating the activation of PI3K-Akt-mTOR signaling pathway on the cell proliferation and apoptosis of osteosarcoma cells through targeting TP53 gene. Eur Rev Med Pharmacol Sci. 2020;24(24):12655–66.
57. Yang Z, Han Y, Cheng K, Zhang G, Wang X. miR-99a directly targets the mTOR signalling pathway in breast cancer side population cells. Cell Prolif. 2014;47(6):587–95.

Publisher's note